Inhibition of CYP2E1 Attenuates Chronic Alcohol Intake-Induced Myocardial Contractile Dysfunction and Apoptosis

Rong-Huai Zhang[1,*], **Jian-Yuan Gao**[1,*], **Hai-Tao Guo**[2], **Glenda I. Scott**[3], **Anna R. Eason**[3], **Xiao-Ming Wang**[1], and **Jun Ren**[1,3]

[1]Department of Geriatrics, Fourth Military Medical University, Xi'an, Shaanxi, PR China

[2]Department of Physiology, Fourth Military Medical University, Xi'an, Shaanxi, PR China

[3]Center for Cardiovascular Research and Alternative Medicine, University of Wyoming College of Health Sciences, Laramie, WY 82071

Abstract

Alcohol intake is associated with myocardial contractile dysfunction and apoptosis although the precise mechanism is unclear. This study was designed to examine the effect of the cytochrome P450 enzyme CYP2E1 inhibition on ethanol-induced cardiac dysfunction. Adult male mice were fed a 4% ethanol liquid or pair-fed control diet for 6 weeks. Following 2 weeks of diet feeding, a cohort of mice started to receive the CYP2E1 inhibitor diallyl sulfide (100 mg/kg/d, i.p.) for the remaining feeding duration. Cardiac function was assessed using echocardiographic and IonOptix systems. Western blot analysis was used to evaluate CYP2E1, heme oxygenase-1 (HO-1), iNOS, the intracellular Ca^{2+} regulatory proteins sarco(endo)plasmic reticulum Ca^{2+}-ATPase, Na^{+}-Ca^{2+} exchanger and phospholamban, pro-apoptotic protein cleaved caspase-3, Bax, c-Jun-NH_2-terminal kinase (JNK) and apoptosis signal-regulating kinase (ASK-1). Ethanol led to elevated levels of CYP2E1, iNOS and phospholamban, decreased levels of HO-1 and Na^{+}-Ca^{2+} exchanger, cardiac contractile and intracellular Ca^{2+} defects, cardiac fibrosis, overt O_2^{-} production, and apoptosis accompanied with increased phosphorylation of JNK and ASK-1, the effects were significantly attenuated or ablated by diallyl sulfide. Inhibitors of JNK and ASK-1 but not HO-1 inducer or iNOS inhibitor obliterated ethanol-induced cardiomyocyte contractile dysfunction, substantiating a role for JNK and ASK-1 signaling in ethanol-induced myocardial injury. Taken together, these findings suggest that ethanol metabolism through CYP2E1 may contribute to the pathogenesis of alcoholic cardiomyopathy including myocardial contractile dysfunction, oxidative stress and apoptosis, possibly through activation of JNK and ASK-1 signaling.

Keywords

CYP2E1; cardiac function; apoptosis; JNK; ASK-1; stress signaling

Correspondence should be addressed to: Dr. Jun Ren, University of Wyoming College of Health Sciences, Laramie, WY 82071, USA; Tel: (307)-766-6131; Fax: (307)-766-2953; jren@uwyo.edu Or Dr. Xiao-Ming Wang, Department of Geriatrics, Fourth Military Medical University, Xi'an 710032, China; Tel: 02984775543; Fax: 02984775543; xmwang@fmmu.edu.cn.
*Equal contribution

1. INTRODUCTION

Chronic ethanol exposure triggers the onset and development of alcoholic cardiomyopathy characterized by disruption of myofibrillary architecture and myocardial contractile dysfunction [1–3]. Although a number of theories have been postulated for ethanol-induced myopathic changes including cardiotoxicity of ethanol and its metabolites, oxidative stress and accumulation of fatty acid ethyl esters [1–4], the ultimate culprit factor(s) behind ethanol-elicited myocardial damage remains elusive. Recent data from our group as well as others have shown a pivotal role of ethanol metabolism in ethanol-induced cell and tissue injuries as well as end organ complications such as alcoholic cardiomyopathy and alcoholic liver diseases [2, 5–8]. In particular, much recent attention has been focused on alcohol dehydrogenase (ADH), aldehyde dehydrogenase (ALDH), cytochrome P450 2E1 (CYP2E1) and catalase enzymes, which catalyze ethanol metabolism [9–11]. Ethanol is metabolized into acetaldehyde by ADH and CYP2E1 in cytoplasm and microsomes, respectively [2]. Convincing evidence from our laboratory as well as others has depicted a rather important role of ADH in the onset and progression of alcoholic cardiomyopathy [12–16]. However, only modest ADH induction was found following chronic ethanol intake as a downstream effect of ethanol inhibiting gonadal hormone production [17]. Earlier findings from our laboratory revealed a likely role of CYP2E1 in ethanol-induced cardiomyocyte contractile defect [18]. CYP2E1 is an enzyme responsible for generation of ROS and reactive metabolites. With alcohol administration, CYP2E1 is induced resulting production of ROS and acetaldehyde to contribute to alcoholic liver diseases [5, 7]. Recent evidence also depicted a unique role of CYP2E1 in isoproterenol-induced cardiac dysfunction [19] although direct evidence for a role of CYP2E1 in alcoholic cardiomyopathy is still lacking.

Given the pivotal role of CYP2E1 in ethanol metabolism and oxidative stress [7], the present study was designed to examine the effect of CYP2E1 inhibitor diallyl sulfide on ethanol intake-induced myocardial contractile dysfunction, intracellular Ca^{2+} derangement and potential signaling mechanisms involved with a focus on apoptotic stress signaling. The organosulfur compound diallyl sulfide has proven effectiveness in prevention of cancer and chemically-induced hepatotoxicity possibly through induction of the cytoprotective protein heme oxygenase-1 (HO-1) as well as suppression of CYP2E1 and inducible nitric oxide synthase (iNOS) [20–21]. Given that apoptotic damage is typical following ethanol challenge, which may play an essential role in ethanol-elicited organ damage [5, 8, 22], apoptosis was assessed using TUNEL staining, caspase-3 activity and protein expression of apoptosis-regulatory proteins. Superoxide (O_2^-) levels and protein carbonyl formation were monitored as an indicator for oxidative stress. As activation of apoptosis signaling-regulated kinase (ASK-1) results in activation of c-Jun-NH_2-terminal kinase (JNK), both of which are known to mediate ethanol-induced hepatic injury via CYP2E1 enzymatic metabolism [23], phosphorylation of JNK and ASK-1 was evaluated in myocardium from ethanol consuming mice with or without diallyl sulfide treatment. To further evaluate the potential role of ASK-1, JNK, HO-1 and iNOS in ethanol-induced cardiac anomalies, ethanol-induced cardiomyocyte contractile response was evaluated in the absence or presence of inhibitors of ASK-1, JNK and iNOS or the HO-1 inducer.

2. MATERIALS AND METHODS

2.1. Chronic ethanol intake and CYP2E1 inhibitor treatment

All animal procedures were conducted in accordance with humane animal care standards outlined in the NIH Guide for the Care and Use of Experimental Animals and were approved the University of Wyoming Animal Care and Use Committee (Laramie, WY). Adult male FVB mice were housed in a temperature-controlled room under a 12hr/12hr-light/dark with access to tap water *ad libitum*. FVB mice were introduced to a nutritionally

complete liquid diet (Shake & Pour Bioserv Inc., Frenchtown, NJ, USA) for a one-week acclimation period. Upon completion of the acclimation period, half of the mice were maintained on the regular liquid diet (without ethanol), and the remaining half began a 6-week period of isocaloric 4% (vol/vol) ethanol diet feeding. An isocaloric pair-feeding regimen was employed to eliminate the possibility of nutritional deficits. Control (non-ethanol consuming) mice were offered the same quantity of diet ethanol-consuming mice drank the previous day [24]. A cohort of ethanol consuming or non-consuming mice were administered the CYP2E1 inhibitor diallyl sulfide (100 mg/kg/d, i.p.) starting from week 3 till the end of diet feeding period [25–26]. Plasma ethanol levels were measured as described [24]. Systolic and diastolic blood pressures were recorded using a CODA non-invasive system (Kent Scientific Co., Torrington, CT).

2.2 Determination of CYP2E1 activity

CYP2E1 activity was assessed using p-nitrophenol (PNP) oxidation to p-nitrocatechol. In brief, ~ 1.5 mg of myocardial microsomal protein was incubated in 1 ml potassium phosphate buffer (100 mM) containing p-nitrophenol (50 μM) with a pH of 6.8. Reaction was initiated with addition of NADPH to a concentration of 0.5 mM and allowed to continue for 10 min at 37°C. Thereafter, 0.5 volume of 0.5 M perchloric acid was added. Proteins were pelleted by centrifugation (4000×g for 15 min). To 1 ml of the supernatant, 100 μl of 10 M NaOH were added, and formed amounts of p-nitrocatechol were measured by spectrophotometry at 511 nm. A calibration curve was constructed by subjecting varying amounts (0–100 nmol) of p-nitrocatechol to the same procedure as the myocardial microsomal preparations [20].

2.3 Echocardiographic assessment

Cardiac geometry and function were evaluated in anesthetized (ketamine 80 mg/kg & xylazine 12 mg/kg, i.p.) mice using a 2-D guided M-mode echocardiography (Sonos 5500) equipped with a 15–6 MHz linear transducer. Left ventricular (LV) wall and chamber dimensions during diastole and systole were recorded from 3 consecutive cycles in M-mode. Fractional shortening was calculated from LV end-diastolic (EDD) and end-systolic (ESD) diameters using the equation (EDD-ESD)/EDD. Cardiac output was calculated from LV end-diastolic and -systolic diameters using the equation $[(LVEDD)^3 - (LVESD)^3]$ x heart rate. Heart rate was calculated from 10 consecutive cardiac cycles [27].

2.4 Cardiomyocyte isolation and in vitro drug treatment

After ketamine/xylazine (80 and 12 mg/kg, respectively, i.p.) sedation, hearts were removed and perfused with KHB buffer containing (in mM): 118 NaCl, 4.7 KCl, 1.2 MgSO$_4$, 1.2 KH$_2$PO$_4$, 25 NaHCO$_3$, 10 HEPES and 11.1 glucose. Hearts were digested with Liberase for 20 min. Left ventricles were removed and minced before being filtered. Cardiomyocyte yield was ~ 75% which was not affected by either ethanol or diallyl sulfide. Only rod-shaped cardiomyocytes with clear edges were used for mechanical evaluation [27]. To examine the potential role of stress signaling, HO-1, and iNOS on ethanol-induced cardiac response, cardiomyocytes from non-ethanol consuming FVB mice were treated with ethanol (240 mg/dl) at 37°C for 4 hrs in the absence or presence of the specific peptide inhibitor of JNK JNKI (2 μM) [28], the ASK-1 inhibitor thioredoxin-1 (50 μM) [23, 29], the HO-1 inducer cobalt protoporphyrin (CoPP, 25 μM) [30] and the specific iNOS inhibitor 1400W (2 μM) [31] prior to the mechanical assessment. The ethanol concentration (240 mg/dl) was chosen largely based on our earlier findings in the cell culture setting [15, 32] and the fact that blood alcohol level may reach 200 mg/dl following chronic drinking in mice [33].

2.5 Cell shortening/relengthening

Mechanical properties of cardiomyocytes were assessed using a SoftEdge MyoCam® system (IonOptix Corporation, Milton, MA, USA). Cells were placed in a chamber mounted on the stage of an inverted microscope (Olympus, IX-70) and superfused (~1 ml/min at 25°C) with a buffer containing (in mM): 131 NaCl, 4 KCl, 1 $CaCl_2$, 1 $MgCl_2$, 10 glucose, 10 HEPES, at pH 7.4. The cells were field stimulated with supra-threshold voltage at a frequency of 0.5 Hz. The myocyte being studied was displayed on the computer monitor using an IonOptix MyoCam camera. An IonOptix SoftEdge software was used to capture changes in cell length during shortening and relengthening. Cell shortening and relengthening were assessed using the following indices: peak shortening (PS) - indicative of ventricular contractility, time-to-PS (TPS) - indicative of contraction duration, and time-to-90% relengthening (TR_{90}) - represents relaxation duration, maximal velocities of shortening (+ dL/dt) and relengthening (–dL/dt) - indicatives of maximal velocities of ventricular pressure rise/fall [27].

2.6 Intracellular Ca^{2+} transients

Cardiomyocytes were loaded with fura-2/AM (0.5 μM) for 15 min, and fluorescence intensity was measured with a dual-excitation fluorescence photomultiplier system (IonOptix). Myocytes were placed on an inverted Olympus microscope and imaged through a Fluor 40x-oil objective. Cells were exposed to light emitted by a 75 W mercury lamp and passed through either a 360 nm or a 380 nm filter. The myocytes were stimulated to contract at 0.5 Hz. Fluorescence emissions were detected between 480 nm and 520 nm by a photomultiplier tube after cells were first illuminated at 360 nm for 0.5 sec and then at 380 nm for the duration of the recording protocol (333 Hz sampling rate). The 360 nm excitation scan was repeated at the end of the protocol, and qualitative changes in intracellular Ca^{2+} concentration were inferred from the ratio of the fluorescence intensity at two wavelengths. Intracellular Ca^{2+} decay rate was calculated from single exponential curve fitting [22].

2.7 Histological examination

Hearts were harvested and sliced at mid-ventricular level followed by fixation with normal buffered formalin. Paraffin-embedded transverse sections were cut in 5-μm in thickness and stained with Masson trichrome. Sections were photographed with a 40× objective of an Olympus BX-51 microscope equipped with an Olympus MaguaFire SP digital camera. Five random fields from each section (3 sections per mouse) were assessed for fibrosis. To determine fibrotic area, pixel counts of blue stained fibers were quantified using Color range and Histogram commands in Photoshop. Fibrotic area was calculated by dividing the pixels of blue stained area to total pixels of non-white area [27].

2.8 TUNEL assay

TUNEL staining of myonuclei positive for DNA strand breaks were determined using a fluorescence detection kit (Roche, Indianapolis, IN, USA) and fluorescence microscopy. Paraffin-embedded sections (5 μm) were incubated with Proteinase K solution for 30 min. TUNEL reaction mixture containing terminal deoxynucleotidyl transferase (TdT) and fluorescein-dUTP was added to the sections in 50-μl drops and incubated for 60 min at 37°C in a humidified chamber in the dark. The sections were rinsed three times in PBS for 5 min each. Following embedding, sections were visualized with an Olympus BX-51 microscope equipped with an Olympus MaguaFire SP digital camera. DNase I and label solution were used as positive and negative controls. To determine the percentage of apoptotic cells, micrographs of TUNEL-positive and DAPI-stained nuclei were captured using an Olympus fluorescence microscope and counted using the ImageJ software (ImageJ version 1.43r;

NIH) followed by manual exclusion of the false-positive staining from 10 random fields at 400× magnification At least 100 cells were counted in each field [27].

2.9 Caspase-3 assay

Tissue homogenates were centrifuged (10,000 g at 4°C, 10 min) and pellets were lysed in an ice-cold cell lysis buffer. The assay was carried out in a 96-well plate with each well containing 30 µl cell lysate, 70 µl of assay buffer (50 mM HEPES, 0.1% CHAPS, 100 mM NaCl, 10 mM DTT and 1 mM EDTA) and 20 µl of caspase-3 colorimetric substrate Ac-DEVD-pNA. The 96-well plate was incubated at 37°C for 1 hr, during which time the caspase in the sample was allowed to cleave the chromophore p-NA from the substrate molecule. Caspase-3 activity was expressed as picomoles of pNA released per µg of protein per minute [34].

2.10 Intracellular fluorescence measurement of superoxide (O_2^-)

Intracellular O_2^- was monitored by changes in fluorescence intensity resulting from intracellular probe oxidation [27]. In brief, cardiomyocytes were loaded with 5 µM dihydroethidium (DHE) (Molecular Probes, Eugene, OR, USA) for 30 min at 37°C and washed with PBS buffer. Cells were sampled randomly using an Olympus BX-51 microscope equipped with an Olympus MagnaFire™ SP digital camera and ImagePro image analysis software (Media Cybernetics, Silver Spring, MD, USA). Fluorescence was calibrated with InSpeck microspheres (Molecular Probes). An average of 100 cells was evaluated using the grid crossing method in 15 visual fields per isolation.

2.11 Protein carbonyl assay

To assess cardiac oxidative damage, protein carbonyl content was determined [35]. In brief, proteins were extracted and minced to prevent proteolytic degradation. Nucleic acids were eliminated by treating the samples with 1% streptomycin sulfate for 15 min, followed by a 10 min centrifugation (11,000 × g). Protein was precipitated by adding an equal volume of 20% TCA to protein (0.5 mg) and centrifuged for 1 min. The TCA solution was removed and the sample resuspended in 10 mM 2,4-dinitrophenylhydrazine (2,4-DNPH) solution. Samples were incubated at room temperature for 15–30 min. Following a 500 µl of 20% TCA addition, samples were centrifuged for 3 min. The supernatant was discarded, the pellet washed in ethanol:ethyl acetate and allowed to incubate at room temperature for 10 min. The samples were centrifuged again for 3 min and the ethanol:ethyl acetate steps repeated 2 more times. The precipitate was resuspended in 6 M guanidine solution, centrifuged for 3 min and insoluble debris removed. The maximum absorbance (360–390 nm) of the supernatant was read against appropriate blanks (water, 2 M HCl) and the carbonyl content was calculated using the molar absorption coefficient of 22,000 $M^{-1}cm^{-1}$.

2.12 Western blot analysis

Myocardial protein was prepared as described [34]. Samples containing equal amount of proteins were separated on 10% SDS-polyacrylamide gels in a minigel apparatus (Mini-PROTEAN II, Bio-Rad) and transferred to nitrocellulose membranes. The membranes were blocked with 5% milk in TBS-T, and were incubated overnight at 4°C with anti-CYP2E1 (1:1,000), anti-HO-1 (1:1,000), anti-iNOS (1:1,000), anti-SERCA2a (1:1,000), anti-Na$^+$-Ca^{2+} exchanger (1:1,000), anti-phospholamban (1:1,000), anti-phosphorylated phospholamban (Ser16, 1:1,000), anti-cleaved caspase-3 (1:1,000), anti-Bax (1:1,000), anti-JNK (1:1,000), anti-phosphorylated JNK (pJNK, Thr183/Tyr185, 1:1,000), anti-ASK-1 (1:1,000), and anti-phosphorylated ASK-1 (pASK-1, Ser83, 1:1,000) antibodies. Anti-SERCA2a was purchased from Affinity BioReagents (Golden, CO, USA). Anti-phospholamban antibody was purchased from Abcam (Cambridge, MA, USA). All other

antibodies were obtained from Cell Signaling Technology (Beverly, MA, USA). After immunoblotting, the film was scanned and the intensity of immunoblot bands was detected with a Bio-Rad Calibrated Densitometer. GAPDH was used as the loading control.

2.13 Data analysis

Data are Mean ± SEM. Difference was calculated by repeated measures analysis of variance (ANOVA) followed by a Tukey's *post hoc* analysis. A p value < 0.05 was considered significant.

3. RESULTS

3.1 General biometric and echocardiographic features as well as CYP2E1, HO-1 and iNOS levels in control and ethanol consuming mice treated with or without diallyl sulfide

Neither ethanol ingestion nor diallyl sulfide treatment altered body and organ weights or organ size (organ-to-body weight ratio). As expected, chronic ethanol ingestion increased blood alcohol level and systolic blood pressure without affecting diastolic blood pressure, the effects of which were unaffected by CYP2E1 inhibition. Heart rate, left ventricular wall thickness and left ventricular EDD were unaffected by chronic ethanol intake or diallyl sulfide treatment, or both. Ethanol intake significantly enlarged LV ESD, suppressed fractional shortening and cardiac output, the effects of which were obliterated by CYP2E1 inhibition. Diallyl sulfide itself did not elicit any notable effect on echocardiographic properties (Table 1). Consistent with previous findings [20, 33, 36–37], chronic ethanol intake significantly upregulated protein expression and enzymatic activity of CYP2E1 and level of iNOS while downregulating the cytoprotective protein HO-1. Although diallyl sulfide itself failed to alter levels of these ethanol-responsive proteins, it abrogated ethanol-elicited changes in CYP2E1, iNOS and HO-1 (Fig. 1).

3.2 CYP2E1 inhibition on ethanol intake-elicited changes in cardiomyocyte contractile and intracellular Ca^{2+} properties

Ethanol intake significantly prolonged the resting cell length, the effect of which was ablated by diallyl sulfide treatment. Diallyl sulfide did not affect resting cell length by itself. Chronic ethanol intake significantly reduced PS and ± dL/dt as well as prolonged TR_{90} without affecting TPS, the effects of which were abolished by the CYP2E1 inhibitor. Diallyl sulfide itself did not elicit any notable effect on cardiomyocyte contractile mechanics (Fig. 2). To better understand the mechanism(s) underneath CYP2E1 inhibition-offered beneficial myocardial effects against ethanol intake, fura-2 fluorescence was monitored to evaluate intracellular Ca^{2+} handling properties. Cardiomyocytes from chronically ethanol-challenged mice displayed a significantly depressed rise of intracellular Ca^{2+} in response to electrical stimulus (ΔFFI) as well as slowed intracellular Ca^{2+} decay associated with unchanged baseline and peak intracellular Ca^{2+}. Although diallyl sulfide itself did not affect intracellular Ca^{2+} properties, it negated ethanol-induced changes in ΔFFI and intracellular Ca^{2+} decay (Fig. 3).

3.3 Ethanol exposure-induced responses in myocardial histology, apoptosis, protein carbonyl formation and mitochondrial O_2^- production

To assess the impact of diallyl sulfide on myocardial histology following ethanol intake, cardiomyocyte cross-sectional area and interstitial fibrosis were examined. Findings from H&E staining revealed that neither ethanol intake nor CYP2E1 inhibition, or both, significantly affected cardiomyocyte transverse cross-section area. Our data from Masson trichrome staining further revealed overt myocardial fibrosis following chronic ethanol intake, the effect of which was significantly attenuated by CYP2E1 inhibition with little effect of diallyl sulfide itself (Fig. 4).

Ethanol intake is often associated with enhanced apoptosis [34]. To assess the impact of diallyl sulfide on cell survival and oxidative stress following ethanol intake, myocardial apoptosis and oxidative stress were evaluated using TUNEL staining, capase-3 assay, mitochondrial O_2^- production and protein carbonyl formation. Our data shown in Fig. 5 revealed that chronic ethanol intake promoted myocardial apoptosis as evidenced by the TUNEL-positive nuclei visualized in fluorescein green (as a percentage of all nuclei stained with DAPI) and capase-3 activity, the effect of which was significantly attenuated by diallyl sulfide. Likewise, chronic ethanol intake significantly promoted O_2^- production and protein carbonyl formation in the heart, which was significantly attenuated or ablated by CYP2E1 inhibition (Fig. 6). The CYP2E1 inhibitor itself did not elicit any overt effect on apoptosis, O_2^- production and protein carbonyl formation.

3.4 Impact of diallyl sulfide on ethanol-induced change in intracellular Ca^{2+} regulator proteins

To explore the possible mechanism behind diallyl sulfide and/or ethanol intake-induced responses on cardiac contractile function and intracellular Ca^{2+} homeostasis, western blot was performed to assess the levels of the essential intracellular Ca^{2+} regulatory proteins SERCA2a, Na^+-Ca^{2+} exchanger and phospholamban. Our data revealed that ethanol intake significantly downregulated Na^+-Ca^{2+} exchanger and upregulated phospholamban expression without affecting SERCA2a level and phospholamban phosphorylation. Although the CYP2E1 inhibitor itself did not affect the levels of these Ca^{2+} regulatory proteins (or phospholamban phosphorylation), it obliterated chronic ethanol intake-induced changes in Na^+-Ca^{2+} exchanger and phospholamban levels without affecting SERCA2a and phospholamban phosphorylation (Fig. 7).

3.5 Diallyl sulfide on ethanol challenge-induced changes in apoptotic protein makers

In line with the findings from TUNEL staining and caspase-3 assay, our results further indicated that ethanol intake significantly increased expression of the pro-apoptotic proteins Bax and cleaved caspase-3 as well as phosphorylation of the pro-apoptotic stress signaling JNK and ASK-1 (absolute or normalized value) without affecting their pan protein expressions. Although diallyl sulfide itself failed to alter the expression or phosphorylation of these pro-apoptotic proteins, it significantly attenuated or ablated ethanol-elicited responses in cleaved caspase-3, Bax, JNK and ASK-1 (Fig. 8).

3.6 Role of JNK and ASK-1 signaling in ethanol-induced cardiomyocyte mechanical responses

To consolidate a role of JNK and ASK-1 in ethanol-induced cardiomyocyte anomalies, we re-examined cardiomyocyte contractile responses in the absence or presence of the selective inhibitors of JNK and ASK-1. Our findings revealed that inhibition of JNK and ASK-1 signaling cascades using the JNK peptide inhibitor JNKI and thioredoxin-1, respectively, abolished acute ethanol exposure-induced depression in peak shortening and $\pm$ dL/dt as well as prolongation in TR_{90} without affecting resting cell length and TPS. Neither JNKI nor thioredoxin-1 affected cardiomyocyte mechanics by themselves (Fig. 9).

3.7 Role of HO-1 and iNOS in ethanol-induced cardiomyocyte mechanical responses

To assess if HO-1 and iNOS play a role in ethanol-induced cardiomyocyte anomalies, we evaluated cardiomyocyte contractile properties in the absence or presence of the HO-1 inducer cobalt protoporphyrin or the specific iNOS inhibitor 1400W. Result depicted in Fig. 10 revealed that neither induction of HO-1 nor inhibition of iNOS significantly affected ethanol exposure-induced cardiomyocyte contractile anomalies (shown as depressed peak

shortening and $\pm$ dL/dt as well as prolonged TR_{90} along with unchanged TPS). Neither cobalt protoporphyrin nor 1400W affected cardiomyocyte mechanics by themselves.

4. DISCUSSION

The major findings of our study revealed that CYP2E1 inhibition rescued against lowered cardiac output, myocardial contractile dysfunction, intracellular Ca^{2+} mishandling and apoptosis following chronic ethanol intake. This is in line with the fact that diallyl sulfide mitigated chronic ethanol intake-induced rise in the level and enzymatic activity of CYP2E1 as reported in the liver [20, 38]. Data from our study revealed elevated myocardial O_2^- production, protein carbonyl formation, myocardial fibrosis and activation of the stress signaling JNK and ASK-1 following ethanol intake, the effects of which were attenuated or mitigated by diallyl sulfide, suggesting a role of oxidative stress, fibrosis and apoptosis in CYP2E1 inhibition-elicited beneficial myocardial effect against ethanol intake. Furthermore, our *in vitro* experiments further supported a role of JNK and ASK-1 in ethanol-elicited cardiac contractile anomalies. Taken together, these observations revealed, for the first time, that ethanol metabolism through CYP2E1 contributes to the development of alcoholic cardiomyopathy, indicating the promises of CYP2E1 inhibition in the management of alcoholic cardiomyopathy.

Development of alcoholic cardiomyopathy is characterized by compromised myocardial pump function [5, 7–8, 22, 28]. Our data revealed that 6 weeks of ethanol intake lowered cardiac output, triggered cardiac contractile dysfunction, intracellular Ca^{2+} derangement, oxidative stress and apoptosis, in a manner similar to our previous reports using either binge drink or longer-term ethanol intake [3, 12–13, 24, 34, 39]. Our six-week ethanol intake regimen failed to reveal cardiac hypertrophy as those seen in longer periods of ethanol intake [16, 23, 29]. This is supported by unchanged resting cardiomyocyte cell length and cross-sectional area. In our hand, chronic ethanol exposure lowered cardiac output, elevated systolic blood pressure without affecting diastolic blood pressure, the effects of which were negated by diallyl sulfide. The discrepancy between cardiac and vascular effects in response to ethanol exposure and diallyl sulfide treatment is not fully clear although it may be speculated that certain hemodynamic or neurohormonal factors (such as neurotransmitters) may contribute to the regulation of cardiovascular function following chronic ethanol exposure.

Excessive ethanol intake is known to trigger oxidative stress and apoptosis via activation of stress signaling [40–41]. This is supported by our findings of elevated O_2^- production, protein carbonyl formation, TUNEL-staining, caspase-3 activity as well as expression of cleaved caspase-12 and Bax in murine hearts following chronic ethanol intake. Enhanced O_2^- and oxidative stress are well known to promote cardiac contractile and intracellular Ca^{2+} abnormalities as well as interstitial fibrosis [42–43]. It has been demonstrated that ethanol may promote free radical generation through direct and indirect mechanisms such as aldehyde oxidase and xanthine oxidase-mediated oxidation, leading to accumulation of O_2^- and oxidative stress [44]. On the other hand, the occurrence of apoptosis such as seen in our study contributes to loss of cardiomyocytes, and may serve as a predictor of adverse outcomes for cardiac diseases and eventually heart failure [43]. Like many other cardiovascular diseases such as atherosclerosis, myocardial ischemia and reperfusion injury, and diabetic cardiomyopathy, apoptosis plays a pivotal role in the pathogenesis of alcoholic cardiomyopathy [43]. In this study, the up-regulated expression of caspase-3 and Bax, as well as increased TUNEL positive cells and caspase-3 activity depicted the presence of a global myocardial apoptosis following chronic ethanol intake. Our intracellular Ca^{2+} results suggested that cardiac mechanical dysfunction following chronic ethanol intake may be underscored by ethanol-induced intracellular Ca^{2+} derangements (decreased ΔFFI and

prolonged intracellular Ca^{2+} decay), consistent with the notion of an essential role for impaired intracellular Ca^{2+} homeostasis in the pathogenesis of alcoholic cardiomyopathy [3, 39]. This is supported by downregulated Na^+-Ca^{2+} exchanger and upregulated levels of the SERCA-inhibitory protein phospholamban following ethanol intake.

Perhaps the most striking piece of findings from our study was that CYP2E1 inhibition attenuated or abolished chronic ethanol intake-induced myocardial anomalies. Although CYP2E1-mediated ethanol metabolism has been proved to play an essential role in alcoholic liver injury [5, 7, 20, 38], our study presented the first piece of evidence that CYP2E1 inhibition is capable of retarding or preventing the progression of alcoholic cardiomyopathy. Several scenarios may be considered to attribute to the beneficial effects of diallyl sulfide against alcoholism. First, diallyl sulfide may elicit its beneficial effects via alleviating free radicals and anti-apoptosis. CYP2E1 inhibition effectively alleviates ethanol intake-induced oxidative stress and apoptosis, *en route* to preserve cardiac function. This is supported by our current finding that diallyl sulfide attenuated ethanol exposure-induced myocardial protein carbonyl formation and that fact that antioxidant protects against development of alcoholic cardiomyopathy [45]. Second, ethanol intake was found to promote phosphorylation of JINK and ASK-1, two pivotal pro-apoptotic signaling molecules. Interestingly, CYP2E1 inhibition ablated or attenuated ethanol-induced phosphorylation of JNK and ASK-1 substantiated a critical role of pro-apoptotic stress signaling in CYP2E1-mediated protection against ethanol-induced cardiac injury. MAP kinases such as JNK have been shown to play an crucial role in CYP2E1-mediated alcoholic hepatic toxicity [46]. Recent evidence has identified ASK-1, a member of MAP kinase kinase kinase (MAP3K), as a upstream signaling molecule for JNK that is activated in response to oxidative stress, ER stress and pro-inflammatory cytokines such as TNF-α [46]. At resting state, ASK-1 may form an inactive complex with reduced thioredoxin, thus making thioredoxin-1 a natural inhibitor for ASK-1 [47]. Our recent study using a chronic ethanol intake regimen revealed activation of ASK-1 in the heart [35], consistent with the present observation. Data from our study revealed that diallyl sulfide negated ethanol exposure-induced changes in myocardial HO-1 and iNOS expression, consistent with those reported in the liver [20]. These findings favored a possible role of HO-1 and iNOS in alcoholic cardiac injury. HO-1 and iNOS are known to be down- and upregulated, respectively, by ethanol exposure [20, 38]. Nonetheless, our finding that HO-1 induction and iNOS inhibition failed to reconcile ethanol exposure-induced cardiomyocyte anomalies does not support a major role of HO-1 and iNOS in alcoholic cardiomyopathy.

In summary, data from our study provided evidence that CYP2E1 inhibition may counteract chronic ethanol intake-induced myocardial contractile dysfunction, intracellular Ca^{2+} mishandling, oxidative stress and apoptosis, favoring a role of cytochrome P-450 in ethanol-elicit alcoholic cardiomyopathy. CYP2E1 is involved in the metabolism of small molecule substrates such as ethanol, drugs and carcinogens [7, 46]. Recent focus on CYP2E1 revolves around its unique ability to metabolize and activate many toxicologically important compounds including ethanol, carbon tetrachloride, acetaminophen, halothane, benzene, and many other halogenated substrates [7, 46]. Toxicity of these small molecules may be exacerbated following induction of CYP2E1 by ethanol exposure while getting reduced by inhibitors of CYP2E1 or CYP2E1 knockout [7, 46]. Moreover, CYP2E1 enzyme in particular hepatic CYP2E1 can be induced by various pathological insults such as type 2 diabetes, obesity and ethanol intoxication, where presence of high CYP2E1 levels within the mitochondria may be deleterious to facilitate the condition of oxidative stress [5, 46]. Data from our present study should shed some lights towards a better understanding of the role of cytochrome P-450 pathway in myocardial pathology under alcoholism and other conditions.

Acknowledgments

Reference List

1. George A, Figueredo VM. Alcoholic cardiomyopathy: a review. Journal of cardiac failure. 2011; 17:844–849. [PubMed: 21962423]

2. Zhang Y, Ren J. ALDH2 in alcoholic heart diseases: molecular mechanism and clinical implications. Pharmacology & therapeutics. 2011; 132:86–95. [PubMed: 21664374]

3. Ren J, Wold LE. Mechanisms of alcoholic heart disease. Therapeutic advances in cardiovascular disease. 2008; 2:497–506. [PubMed: 19124444]

4. Patel VB, Why HJ, Richardson PJ, Preedy VR. The effects of alcohol on the heart. Adverse drug reactions and toxicological reviews. 1997; 16:15–43. [PubMed: 9192055]

5. Cederbaum AI, Lu Y, Wu D. Role of oxidative stress in alcohol-induced liver injury. Archives of toxicology. 2009; 83:519–548. [PubMed: 19448996]

6. Guo R, Zhong L, Ren J. Overexpression of aldehyde dehydrogenase-2 attenuates chronic alcohol exposure-induced apoptosis, change in Akt and Pim signalling in liver. Clinical and experimental pharmacology & physiology. 2009; 36:463–468. [PubMed: 19215238]

7. Knockaert L, Fromenty B, Robin MA. Mechanisms of mitochondrial targeting of cytochrome P450 2E1: physiopathological role in liver injury and obesity. The FEBS journal. 2011; 278:4252–4260. [PubMed: 21929725]

8. Cohen JI, Chen X, Nagy LE. Redox signaling and the innate immune system in alcoholic liver disease. Antioxidants & redox signaling. 2011; 15:523–534. [PubMed: 21126203]

9. Manzo-Avalos S, Saavedra-Molina A. Cellular and mitochondrial effects of alcohol consumption. Int J Environ Res Public Health. 2010; 7:4281–4304. [PubMed: 21318009]

10. Wu D, Cederbaum AI. Oxidative stress and alcoholic liver disease. Semin Liver Dis. 2009; 29:141–154. [PubMed: 19387914]

11. Wu D, Wang X, Zhou R, Cederbaum A. CYP2E1 enhances ethanol-induced lipid accumulation but impairs autophagy in HepG2 E47 cells. Biochem Biophys Res Commun. 2010; 402:116–122. [PubMed: 20932821]

12. Guo R, Hu N, Kandadi MR, Ren J. Facilitated ethanol metabolism promotes cardiomyocyte contractile dysfunction through autophagy in murine hearts. Autophagy. 2012; 8

13. Guo R, Scott GI, Ren J. Involvement of AMPK in alcohol dehydrogenase accentuated myocardial dysfunction following acute ethanol challenge in mice. PloS one. 2010; 5:e11268. [PubMed: 20585647]

14. Ren J. Acetaldehyde and alcoholic cardiomyopathy: lessons from the ADH and ALDH2 transgenic models. Novartis Foundation symposium. 2007; 285:69–76. discussion 76-69, 198–199. [PubMed: 17590987]

15. Duan J, McFadden GE, Borgerding AJ, Norby FL, Ren BH, Ye G, Epstein PN, Ren J. Overexpression of alcohol dehydrogenase exacerbates ethanol-induced contractile defect in cardiac myocytes. American journal of physiology Heart and circulatory physiology. 2002; 282:H1216–1222. [PubMed: 11893554]

16. Liang Q, Carlson EC, Borgerding AJ, Epstein PN. A transgenic model of acetaldehyde overproduction accelerates alcohol cardiomyopathy. The Journal of pharmacology and experimental therapeutics. 1999; 291:766–772. [PubMed: 10525098]

17. Rachamin G, MacDonald JA, Wahid S, Clapp JJ, Khanna JM, Israel Y. Modulation of alcohol dehydrogenase and ethanol metabolism by sex hormones in the spontaneously hypertensive rat. Effect of chronic ethanol administration. Biochem J. 1980; 186:483–490. [PubMed: 6990919]

18. Aberle NS 2nd, Ren J. Short-term acetaldehyde exposure depresses ventricular myocyte contraction: role of cytochrome P450 oxidase, xanthine oxidase, and lipid peroxidation. Alcoholism, clinical and experimental research. 2003; 27:577–583.

19. Zordoky BN, Aboutabl ME, El-Kadi AO. Modulation of cytochrome P450 gene expression and arachidonic acid metabolism during isoproterenol-induced cardiac hypertrophy in rats. Drug

metabolism and disposition: the biological fate of chemicals. 2008; 36:2277–2286. [PubMed: 18725507]

20. Shaik IH, George JM, Thekkumkara TJ, Mehvar R. Protective effects of diallyl sulfide, a garlic constituent, on the warm hepatic ischemia-reperfusion injury in a rat model. Pharm Res. 2008; 25:2231–2242. [PubMed: 18626753]

21. Kalayarasan S, Sriram N, Sudhandiran G. Diallyl sulfide attenuates bleomycin-induced pulmonary fibrosis: critical role of iNOS, NF-kappaB, TNF-alpha and IL-1beta. Life Sci. 2008; 82:1142–1153. [PubMed: 18462759]

22. Turdi S, Kandadi MR, Zhao J, Huff AF, Du M, Ren J. Deficiency in AMP-activated protein kinase exaggerates high fat diet-induced cardiac hypertrophy and contractile dysfunction. Journal of molecular and cellular cardiology. 2011; 50:712–722. [PubMed: 21167835]

23. Yang L, Wu D, Wang X, Cederbaum AI. Depletion of cytosolic or mitochondrial thioredoxin increases CYP2E1-induced oxidative stress via an ASK-1-JNK1 pathway in HepG2 cells. Free radical biology & medicine. 2011; 51:185–196. [PubMed: 21557999]

24. Hintz KK, Relling DP, Saari JT, Borgerding AJ, Duan J, Ren BH, Kato K, Epstein PN, Ren J. Cardiac overexpression of alcohol dehydrogenase exacerbates cardiac contractile dysfunction, lipid peroxidation, and protein damage after chronic ethanol ingestion. Alcoholism, clinical and experimental research. 2003; 27:1090–1098.

25. Grudzinski IP, Frankiewicz-Jozko A, Bany J. Diallyl sulfide--a flavour component from garlic (Allium sativum) attenuates lipid peroxidation in mice infected with Trichinella spiralis. Phytomedicine : international journal of phytotherapy and phytopharmacology. 2001; 8:174–177. [PubMed: 11417909]

26. Lin X, Yu S, Chen Y, Wu J, Zhao J, Zhao Y. Neuroprotective effects of diallyl sulfide against transient focal cerebral ischemia via anti-apoptosis in rats. Neurological research. 2012; 34:32–37. [PubMed: 22196859]

27. Zhang Y, Li L, Hua Y, Nunn JM, Dong F, Yanagisawa M, Ren J. Cardiac-specific knockout of ETA receptor mitigates low ambient temperature-induced cardiac hypertrophy and contractile dysfunction. Journal of molecular cell biology. 2012

28. Turdi S, Yuan M, Leedy GM, Wu Z, Ren J. Chronic social stress induces cardiomyocyte contractile dysfunction and intracellular Ca2+ derangement in rats. Physiology & behavior. 2012; 105:498–509. [PubMed: 21952229]

29. Tao L, Jiao X, Gao E, Lau WB, Yuan Y, Lopez B, Christopher T, RamachandraRao SP, Williams W, Southan G, Sharma K, Koch W, Ma XL. Nitrative inactivation of thioredoxin-1 and its role in postischemic myocardial apoptosis. Circulation. 2006; 114:1395–1402. [PubMed: 16966583]

30. Kawamoto S, Flynn JP, Shi Q, Sakr SW, Luo J, Allen MD. Heme oxygenase-1 induction enhances cell survival and restores contractility to unvascularized three-dimensional adult cardiomyocyte grafts implanted in vivo. Tissue Eng Part A. 2011; 17:1605–1614. [PubMed: 21288159]

31. Li S, Jiao X, Tao L, Liu H, Cao Y, Lopez BL, Christopher TA, Ma XL. Tumor necrosis factor-alpha in mechanic trauma plasma mediates cardiomyocyte apoptosis. American journal of physiology Heart and circulatory physiology. 2007; 293:H1847–1852. [PubMed: 17616742]

32. Duan J, Esberg LB, Ye G, Borgerding AJ, Ren BH, Aberle NS, Epstein PN, Ren J. Influence of gender on ethanol-induced ventricular myocyte contractile depression in transgenic mice with cardiac overexpression of alcohol dehydrogenase. Comp Biochem Physiol A Mol Integr Physiol. 2003; 134:607–614. [PubMed: 12600669]

33. Matson L, Liangpunsakul S, Crabb D, Buckingham A, Ross RA, Halcomb M, Grahame N. Chronic Free-Choice Drinking in Crossed High Alcohol Preferring Mice Leads to Sustained Blood Ethanol Levels and Metabolic Tolerance Without Evidence of Liver Damage. Alcoholism, clinical and experimental research. 2012

34. Guo R, Ren J. Alcohol dehydrogenase accentuates ethanol-induced myocardial dysfunction and mitochondrial damage in mice: role of mitochondrial death pathway. PloS one. 2010; 5:e8757. [PubMed: 20090911]

35. Doser TA, Turdi S, Thomas DP, Epstein PN, Li SY, Ren J. Transgenic overexpression of aldehyde dehydrogenase-2 rescues chronic alcohol intake-induced myocardial hypertrophy and contractile dysfunction. Circulation. 2009; 119:1941–1949. [PubMed: 19332462]

36. Sebastian BM, Roychowdhury S, Tang H, Hillian AD, Feldstein AE, Stahl GL, Takahashi K, Nagy LE. Identification of a cytochrome P4502E1/Bid/C1q-dependent axis mediating inflammation in adipose tissue after chronic ethanol feeding to mice. J Biol Chem. 2011; 286:35989–35997. [PubMed: 21856753]

37. Dantas AM, Mohn CE, Burdet B, Zubilete MZ, Mandalunis PM, Elverdin JC, Fernandez-Solari J. Ethanol consumption enhances periodontal inflammatory markers in rats. Arch Oral Biol. 2012

38. Ronis MJ, Korourian S, Blackburn ML, Badeaux J, Badger TM. The role of ethanol metabolism in development of alcoholic steatohepatitis in the rat. Alcohol. 2010; 44:157–169. [PubMed: 20116195]

39. Zhang B, Turdi S, Li Q, Lopez FL, Eason AR, Anversa P, Ren J. Cardiac overexpression of insulin-like growth factor 1 attenuates chronic alcohol intake-induced myocardial contractile dysfunction but not hypertrophy: Roles of Akt, mTOR, GSK3beta, and PTEN. Free radical biology & medicine. 2010; 49:1238–1253. [PubMed: 20678571]

40. Hajnoczky G, Buzas CJ, Pacher P, Hoek JB, Rubin E. Alcohol and mitochondria in cardiac apoptosis: mechanisms and visualization. Alcoholism, clinical and experimental research. 2005; 29:693–701.

41. Lieber CS. Microsomal ethanol-oxidizing system (MEOS): the first 30 years (1968–1998)--a review. Alcoholism, clinical and experimental research. 1999; 23:991–1007.

42. Tsutsui H, Kinugawa S, Matsushima S. Mitochondrial oxidative stress and dysfunction in myocardial remodelling. Cardiovascular research. 2009; 81:449–456. [PubMed: 18854381]

43. Tsutsui H, Kinugawa S, Matsushima S. Oxidative stress and heart failure. American journal of physiology Heart and circulatory physiology. 2011; 301:H2181–2190. [PubMed: 21949114]

44. McDonough KH. The role of alcohol in the oxidant antioxidant balance in heart. Frontiers in bioscience : a journal and virtual library. 1999; 4:D601–606. [PubMed: 10417058]

45. Li Q, Ren J. Cardiac overexpression of metallothionein attenuates chronic alcohol intake-induced cardiomyocyte contractile dysfunction. Cardiovasc Toxicol. 2006; 6:173–182. [PubMed: 17347528]

46. Cederbaum AI, Yang L, Wang X, Wu D. CYP2E1 Sensitizes the Liver to LPS- and TNF alpha-Induced Toxicity via Elevated Oxidative and Nitrosative Stress and Activation of ASK-1 and JNK Mitogen-Activated Kinases. International journal of hepatology. 2012; 2012:582790. [PubMed: 22028977]

47. Fujino G, Noguchi T, Matsuzawa A, Yamauchi S, Saitoh M, Takeda K, Ichijo H. Thioredoxin and TRAF family proteins regulate reactive oxygen species-dependent activation of ASK1 through reciprocal modulation of the N-terminal homophilic interaction of ASK1. Molecular and cellular biology. 2007; 27:8152–8163. [PubMed: 17724081]
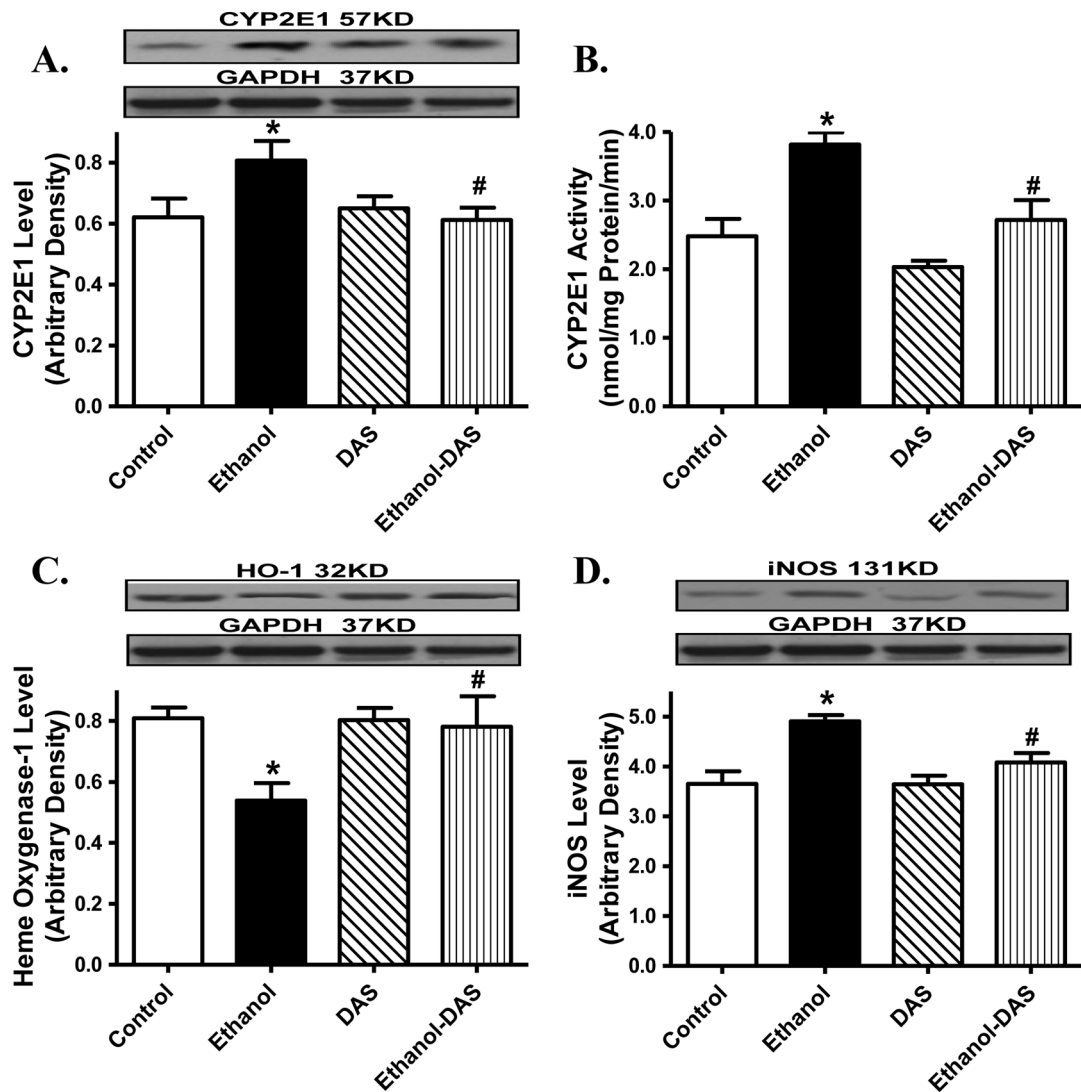
Research highlights

- We examine the effect of CYP2E1 inhibition against alcoholic cardiomyopathy;

- Diallyl sulfide alleviates ethanol intake-induced cardiac defect and apoptosis;

- CYP2E1 inhibition inhibits oxidative stress, activation of ASK-1 and JNK;

Fig. 1.
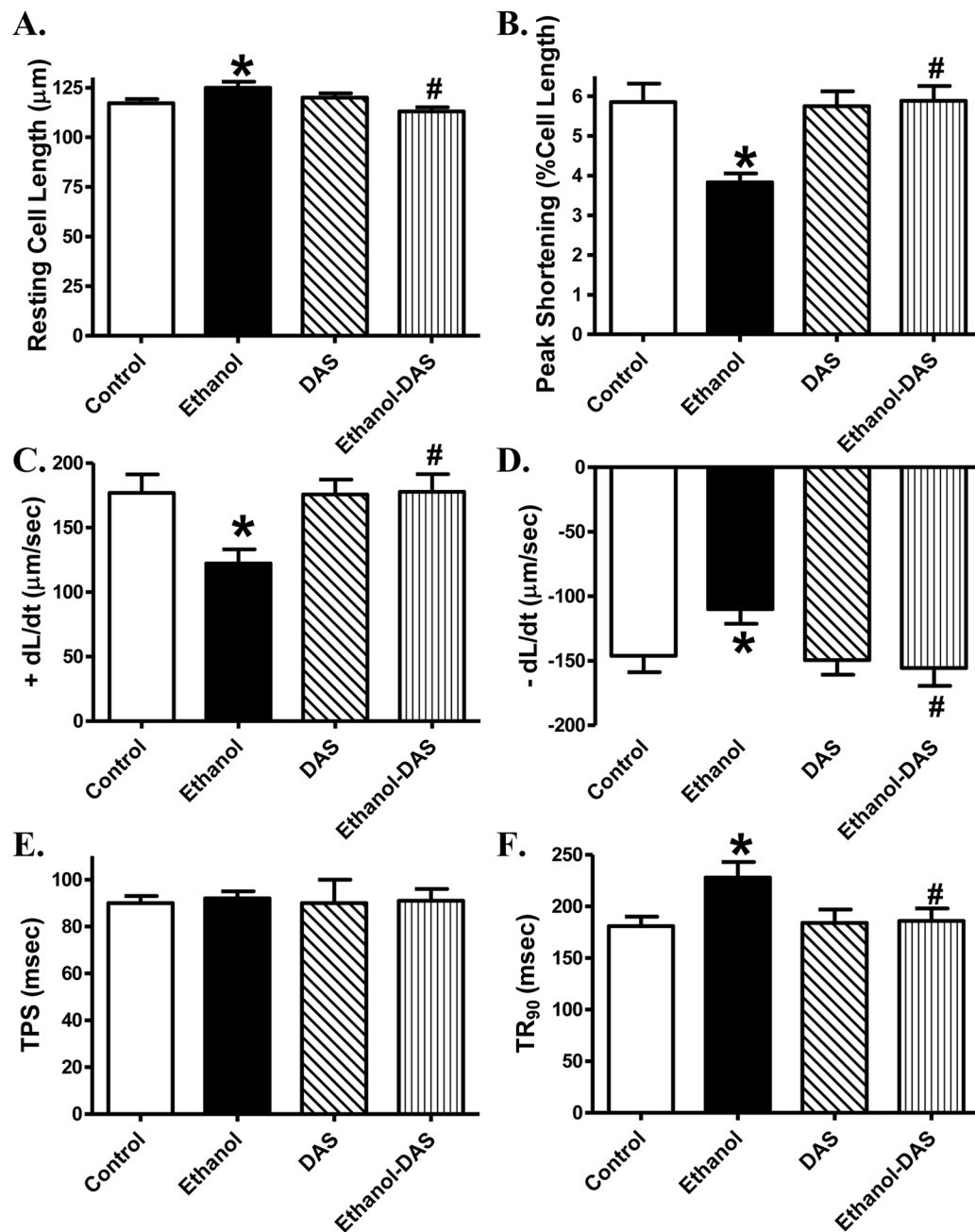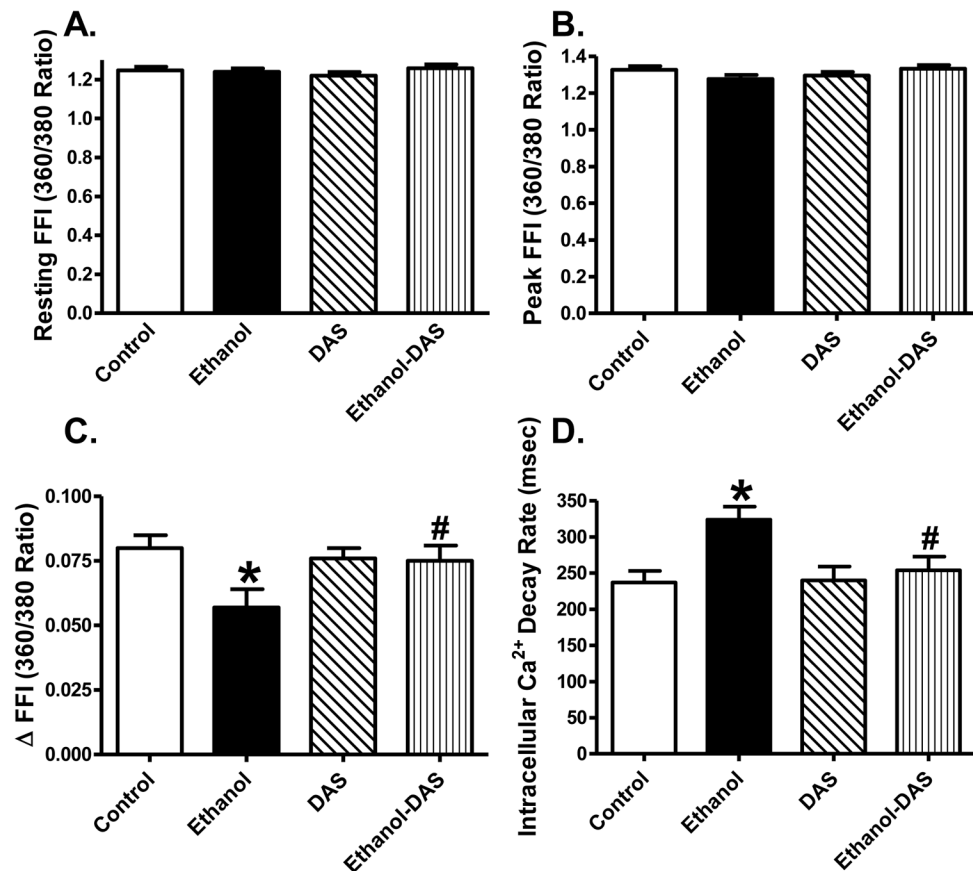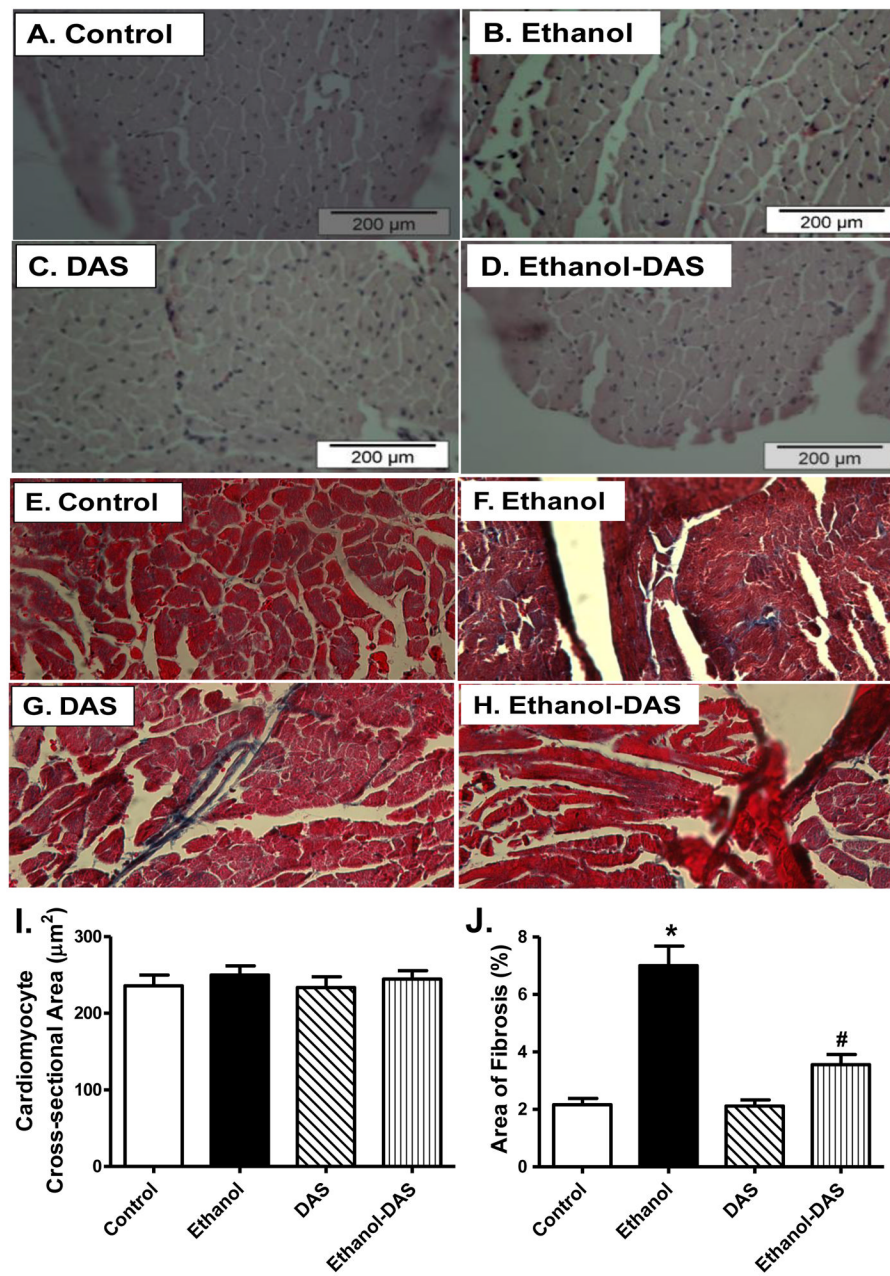Effect of the CYP2E1 inhibitor diallyl sulfide (DAS, 100 mg/kg/d, i.p., for 4 weeks) on ethanol intake-induced changes in myocardial level and/or activity of CYP2E1, heme oxygenase-1 (HO-1) and iNOS. Mice were fed control or ethanol (4%) diet for 6 weeks prior to collection of tissues for Western blot analysis. Cohorts of ethanol consuming or non-consuming mice were administered DAS (week 3–6). A: CYP2E1 level; B: CYP2E1 activity; C: HO-1 level; and D: iNOS level; Insets: Representative gels depicting levels of CYP2E1, HO-1 and iNOS using specific antibodies. GAPDH was used as the loading control. Mean ± SEM, n = 4 – 6 mice per group, * p < 0.05 *vs.* control group, # p < 0.05 *vs.* ethanol group.
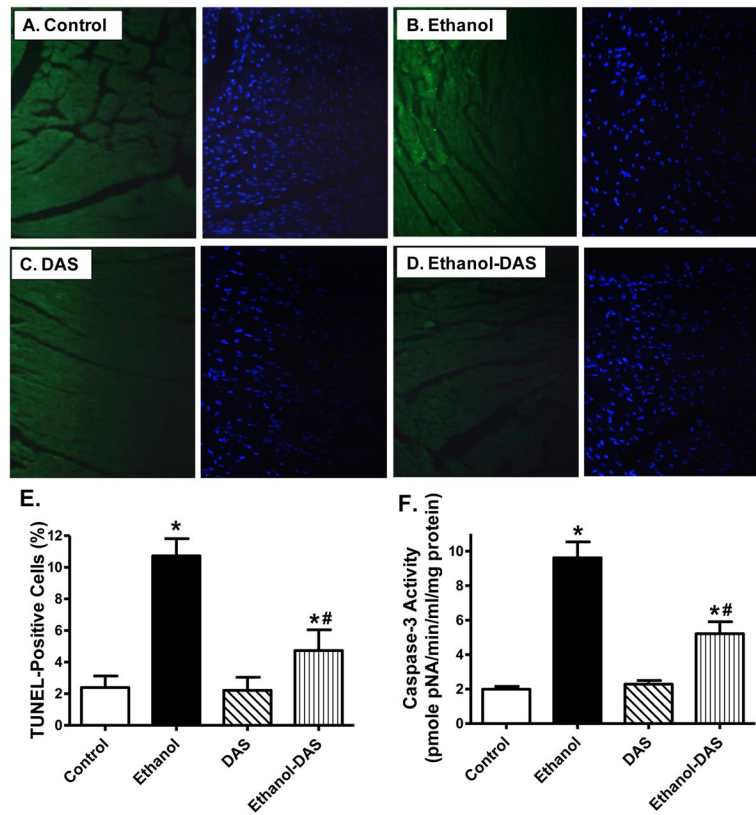
Fig. 2.
Effect of the CYP2E1 inhibitor diallyl sulfide (DAS, 100 mg/kg/d, i.p., for 4 weeks) on ethanol intake-induced cardiomyocyte contractile dysfunction. Mice were fed control or ethanol (4%) diet for 6 weeks prior to mechanical assessment. Cohorts of ethanol consuming or non-consuming mice were administered DAS stating from week 3 till the end of feeding period. A: Resting cell length; B: Peak shortening (PS, normalized to cell length); C: Maximal velocity of shortening (+ dL/dt); D: Maximal of relengthening (− dL/dt); E: Time-to-PS (TPS) and F: Time-to-90% relengthening (TR$_{90}$). Mean ± SEM, n = 103 cells from 4 mice per group, * p < 0.05 *vs.* control group, # p < 0.05 *vs.* ethanol group.
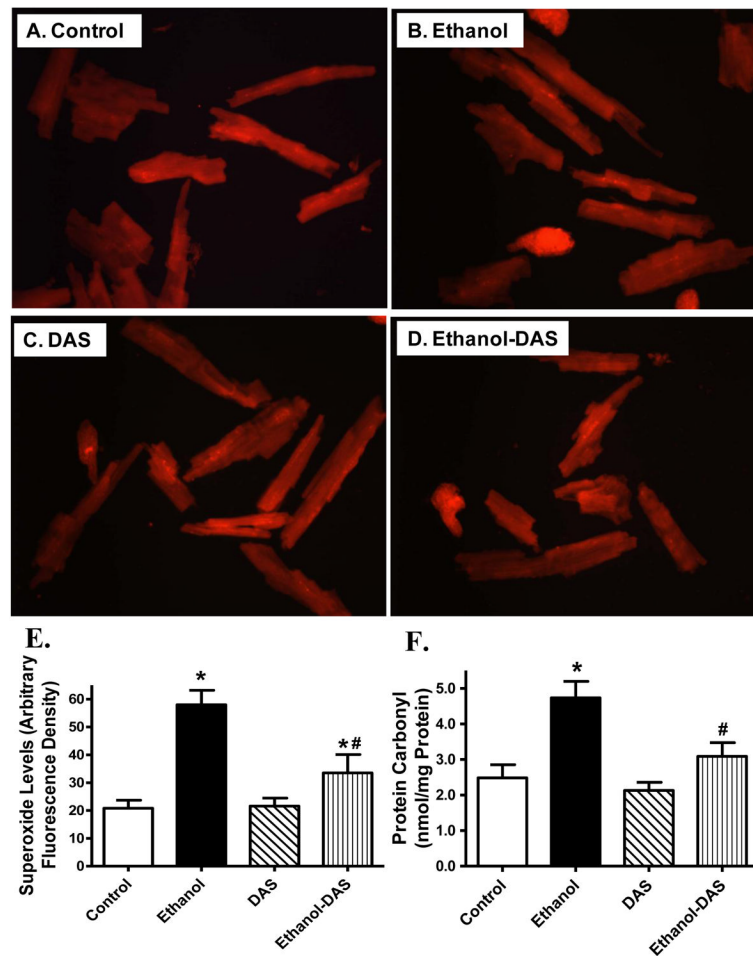
Fig. 3.
Effect of the CYP2E1 inhibitor diallyl sulfide (DAS, 100 mg/kg/d, i.p., for 4 weeks) on ethanol intake-induced intracellular Ca^{2+} handling derangement. Mice were fed control or ethanol (4%) diet for 6 weeks prior to intracellular Ca^{2+} measurement. Cohorts of ethanol consuming or non-consuming mice were administered DAS stating from week 3 till the end of feeding period. A: Resting fura-2 fluorescence intensity (FFI); B: Peak FFI; C: Electrically-stimulated rise in FFI (ΔFFI); and D: Intracellular Ca^{2+} decay rate. Mean ± SEM, n = 91 – 92 cells from 4 mice per group, * p < 0.05 *vs.* control group, # p < 0.05 *vs.* ethanol group.
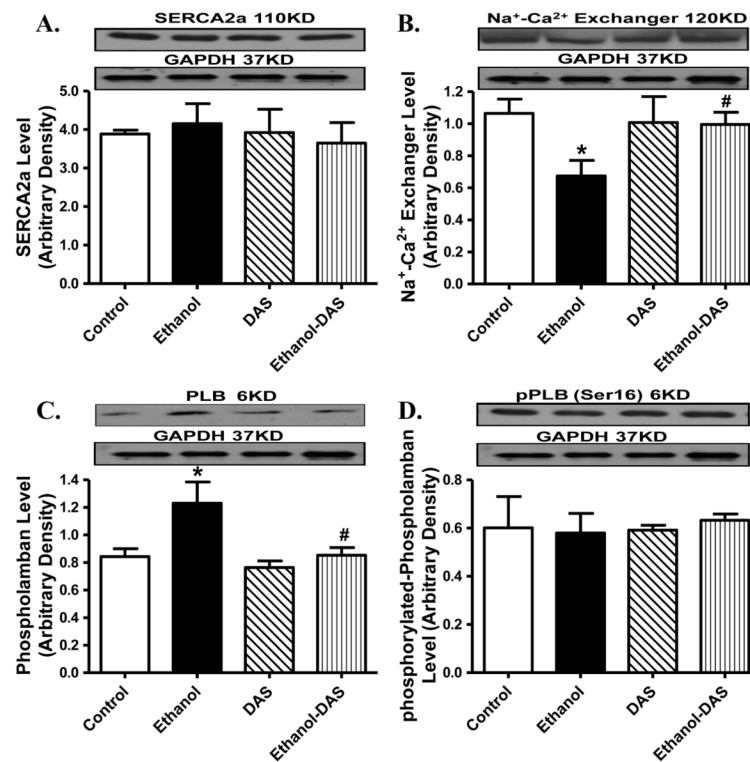
Fig. 4.
Effect of the CYP2E1 inhibitor diallyl sulfide (DAS, 100 mg/kg/d, i.p., for 4 weeks) on ethanol intake-induced histological changes. Mice were fed control or ethanol (4%) diet for 6 weeks prior to histological assessment. Cohorts of ethanol consuming or non-consuming mice were administered DAS (week 3–6). A-D: Representative H&E micrographs depicting cross-sections of left ventricles (x 200); E-H: Representative Masson Trichrome micrographs showing longitudinal sections of left ventricles (x 400); I: Quantitative analysis of cardiomyocyte cross-sectional area from 43 fields; and J: Quantitative analysis of fibrotic area (Masson trichrome stained area in light blue color normalized to total myocardial area) from ~ 50 sections from 4 mice per group; Mean ± SEM, * $p < 0.05$ *vs.* control group, # $p < 0.05$ *vs.* ethanol group.
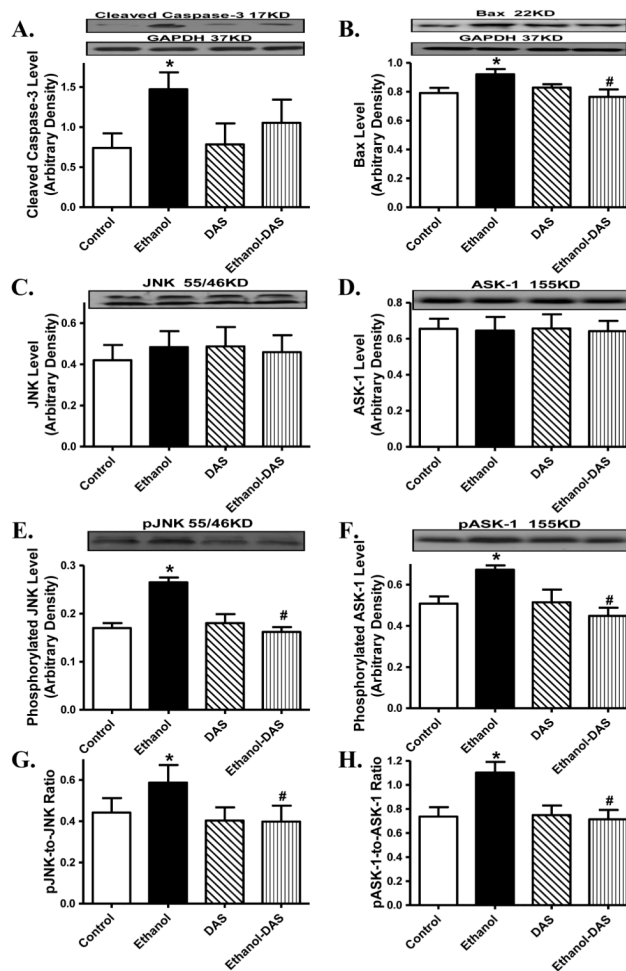
Fig. 5.
Effect of the CYP2E1 inhibitor diallyl sulfide (DAS, 100 mg/kg/d, i.p., for 4 weeks) on ethanol intake-induced myocardial apoptosis. Mice were fed control or ethanol (4%) diet for 6 weeks prior to assessment of apoptosis. A–D: Photomicrograph showing TUNEL staining in myocardium from mice fed control or ethanol diet with or without DAS treatment. TUNEL positive nuclei were visualized with fluorescein (green). A: Control; C: Ethanol; C: DAS; and D: Ethanol-DAS. All nuclei were stained with DAPI shown in blue color; E: Pooled data of TUNEL staining; and F: Myocardial caspase-3 activity. Mean ± SEM, n = 9 fields (panel E) or 7–8 hearts (panel F) per group, * p < 0.05 *vs.* control group, # p < 0.05 *vs.* ethanol group.

Fig. 6.
Effect of the CYP2E1 inhibitor diallyl sulfide (DAS, 100 mg/kg/d, i.p., for 4 weeks) on ethanol intake-induced O_2^- production and protein carbonyl formation. Mice were fed control or ethanol (4%) diet for 6 weeks prior to assessment of DHE fluorescence. Cohorts of ethanol consuming or non-consuming mice were administered DAS stating from week 3. A–D: Representative fluorescence images (40x) from control, ethanol, DAS and ethanol-DAS groups; E: Pooled data; and F: Protein carbonyl level. Mean ± SEM, n = 9 fields (panel E) or 7 mice (panel F) per group, * p < 0.05 *vs.* control group, # p < 0.05 *vs.* ethanol group.

Fig. 7.
Effect of the CYP2E1 inhibitor diallyl sulfide (DAS, 100 mg/kg/d, i.p., for 4 weeks) on ethanol intake-induced changes in intracellular Ca^{2+} regulatory proteins. Mice were fed control or ethanol (4%) diet for 6 weeks prior to collection of tissues for Western blot analysis. Cohorts of ethanol consuming or non-consuming mice were administered DAS stating from week 3. A: SERCA2a; B: Na^+-Ca^{2+} exchanger; C: Phospholamban; and D: phosphorylated phospholamban; Insets: Representative gels depicting intracellular Ca^{2+} regulatory proteins using specific antibodies. GAPDH was used as the loading control. Mean ± SEM, n = 4 – 6 mice per group, * p < 0.05 *vs.* control group, # p < 0.05 *vs.* ethanol group.

Fig. 8.
Effect of the CYP2E1 inhibitor diallyl sulfide (DAS, 100 mg/kg/d, i.p., for 4 weeks) on ethanol intake-induced changes in pro-apoptotic stress signaling. Mice were fed control or ethanol (4%) diet for 6 weeks prior to collection of tissues for Western blot analysis. Cohorts of ethanol consuming or non-consuming mice were administered DAS (week 3–6). A: Cleaved caspase-3; B: Bax; C: JNK; D: ASK-1; E: phosphorylated JNK (pJNK); F: phosphorylated ASK-1 (pASK-1); G: pJNK-to-JNK ratio; and H: pASK-1-to-ASK-1 ratio; Insets: Representative gels depicting pro-apoptotic proteins using specific antibodies. GAPDH was used as the loading control. Mean ± SEM, n = 5 – 7 mice per group, * p < 0.05 *vs.* control group, # p < 0.05 *vs.* ethanol group.
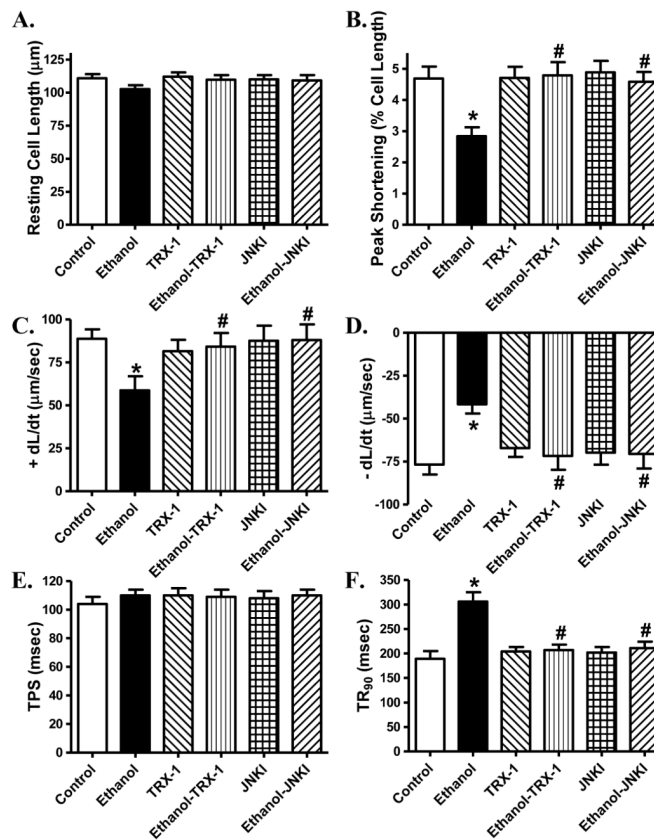
Fig. 9.
Effect of the ASK-1 inhibitor thioredoxin-1 (TRX-1, 50 μM) and the JNK specific peptide
inhibitor JNKI (2 μM) on ethanol exposure (240 mg/dl, 4 hrs)-induced cardiomyocyte
contractile dysfunction. A: Resting cell length; B: Peak shortening (PS, normalized to cell
length); C: Maximal velocity of shortening (+ dL/dt); D: Maximal of relengthening (− dL/
dt); E: Time-to-PS (TPS) and F: Time-to-90% relengthening (TR$_{90}$). Mean ± SEM, n = 50
cells from 2 mice per group, * p < 0.05 *vs.* control group, # p < 0.05 *vs.* ethanol group.
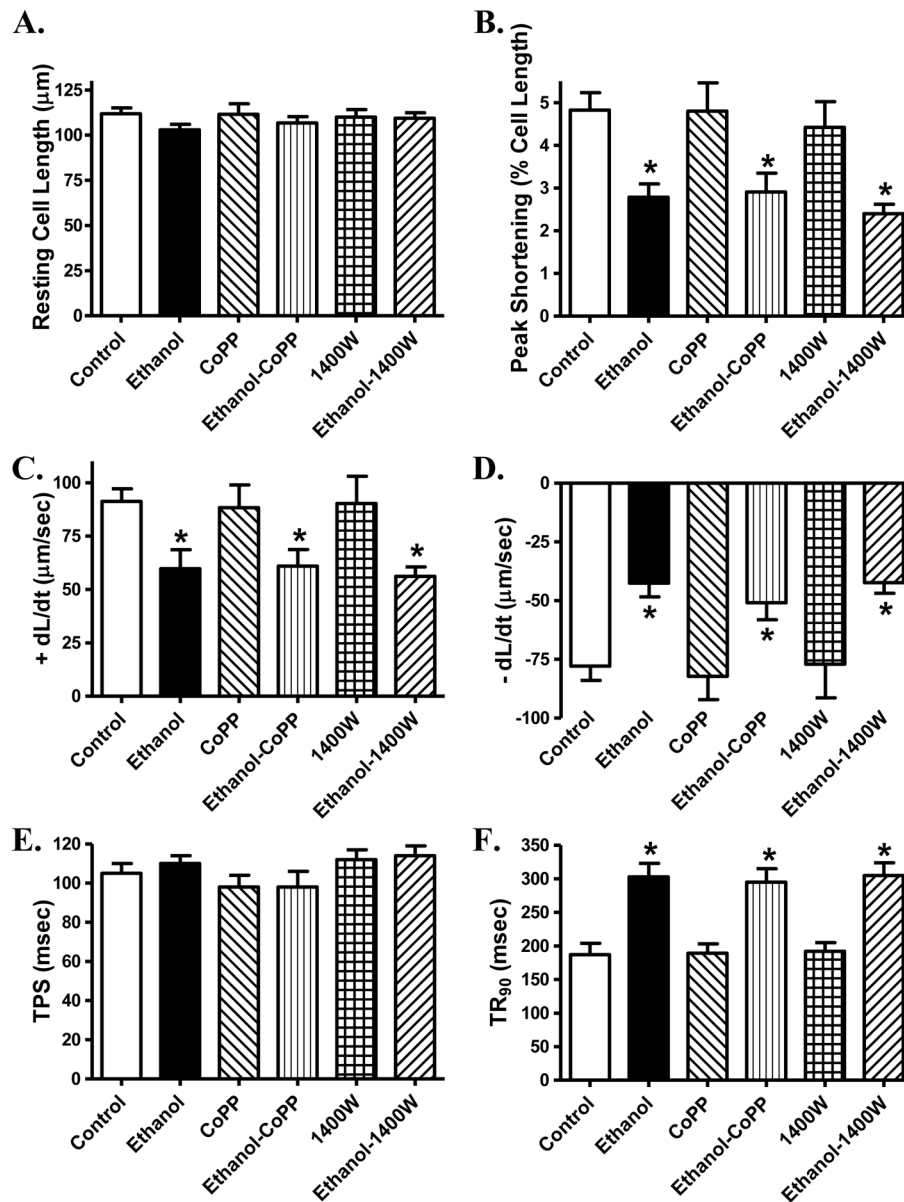
Fig. 10.
Effect of the HO-1 inducer cobalt protoporphyrin (CoPP, 25 μM) and the iNOS inhibitor 1400W (2 μM) on ethanol exposure (240 mg/dl, 4 hrs)-induced cardiomyocyte contractile dysfunction. A: Resting cell length; B: Peak shortening (PS, normalized to cell length); C: Maximal velocity of shortening (+ dL/dt); D: Maximal of relengthening (− dL/dt); E: Time-to-PS (TPS) and F: Time-to-90% relengthening (TR_{90}). Mean ± SEM, n = 46 cells from 2 mice per group, * $p < 0.05$ *vs.* control group.

Table 1

Biometric and echocardiographic parameters of control and alcohol consuming mice

Parameter	Control	Ethanol	DAS	Ethanol-DAS
Body Weight (g)	25.2 ± 0.6	25.6 ± 0.7	24.9 ± 0.5	25.6 ± 0.5
Heart Weight (mg)	140 ± 5	140 ± 4	138 ± 5	141 ± 4
Heart/Body Weight (mg/g)	5.57 ± 0.19	5.51 ± 0.13	5.56 ± 0.16	5.49 ± 0.07
Liver Weight (g)	1.31 ± 0.05	1.32 ± 0.02	1.31 ± 0.03	1.34 ± 0.03
Liver/Body Weight (mg/g)	51.8 ± 1.5	51.9 ± 2.1	52.7 ± 1.2	52.3 ± 0.8
Kidney Weight (mg)	317 ± 10	324 ± 15	314 ± 10	333 ± 12
Kidney/Body Weight (mg/g)	12.6 ± 0.3	12.7 ± 0.6	12.6 ± 0.3	13.0 ± 0.4
Diastolic Blood Pressure (mmHg)	79.4 ± 1.9	78.7 ± 1.8	78.4 ± 1.8	79.0 ± 1.7
Systolic Blood Pressure (mmHg)	112.2 ± 2.1	125.2 ± 2.2*	109.9 ± 2.1	125.1 ± 2.7*
Blood Alcohol Level (mg/dl)	Undetectable	73.2 ± 4.5*	Undetectable	77.2 ± 4.8*
Heart Rate (bpm)	451 ± 12	447 ± 12	460 ± 13	460 ± 12
LV Wall Thickness (mm)	0.98 ± 0.03	0.95 ± 0.04	0.94 ± 0.03	0.95 ± 0.04
LV ESD (mm)	1.29 ± 0.05	1.53 ± 0.04*	1.34 ± 0.04	1.33 ± 0.06#
LV EDD (mm)	2.56 ± 0.11	2.44 ± 0.04	2.61 ± 0.11	2.56 ± 0.15
Factional Shortening (%)	49.3 ± 1.7	37.1 ± 1.5*	47.7 ± 1.9	47.5 ± 1.5#
Cardiac Output (mm³ * min)	7447 ± 926	4939 ± 357*	7434 ± 914	7563 ± 1221#

LV: left ventricular; LV ESD: LV end systolic diameter; LV EDD: LV end diastolic diameter;

Mean ± SEM, n = 9 – 10 mice per group, undetectable: < 2.5 mg/dl,

*
p < 0.05 *vs.* control group,

#
p < 0.05 *vs.* ethanol group.